Editors' Suggestion

Spiral wave drift under optical feedback in cardiac tissue

Yuan-Xun Xia,[1] Xin-Pei Zhi,[1] Teng-Chao Li,[2] Jun-Ting Pan,[3] Alexander V. Panfilov,[4,5,6,*] and Hong Zhang[1,†]

[1]*Zhejiang Institute of Modern Physics, School of Physics, Zhejiang University, Hangzhou 310027, China*
[2]*School of Physics and Telecommunication Engineering, South China Normal University, Guangzhou 510006, China*
[3]*Ocean College, Zhejiang University, Zhoushan 316021, China*
[4]*Department of Physics and Astronomy, Ghent University, Ghent 9000, Belgium*
[5]*Laboratory of Computational Biology and Medicine, Ural Federal University, Ekaterinburg 620002, Russia*
[6]*World-Class Research Center "Digital Biodesign and Personalized Healthcare", Sechenov University, Moscow 119146, Russia*

(Received 3 November 2021; revised 3 April 2022; accepted 1 June 2022; published 8 August 2022)

Spiral waves occur in various types of excitable media and their dynamics determine the spatial excitation patterns. An important type of spiral wave dynamics is drift, as it can control the position of a spiral wave or eliminate a spiral wave by forcing it to the boundary. In theoretical and experimental studies of the Belousov-Zhabotinsky reaction, it was shown that the most direct way to induce the controlled drift of spiral waves is by application of an external electric field. Mathematically such drift occurs due to the onset of additional gradient terms in the Laplacian operator describing excitable media. However, this approach does not work for cardiac excitable tissue, where an external electric field does not result in gradient terms. In this paper, we propose a method of how to induce a directed linear drift of spiral waves in cardiac tissue, which can be realized as an optical feedback control in tissue where photosensitive ion channels are expressed. We illustrate our method by using the FitzHugh-Nagumo model for cardiac tissue and the generic model of photosensitive ion channels. We show that our method works for continuous and discrete light sources and can effectively move spiral waves in cardiac tissue, or eliminate them by collisions with the boundary or with another spiral wave. We finally implement our method by using a biophysically motivated photosensitive ion channel model included to the Luo-Rudy model for cardiac cells and show that the proposed feedback control also induces directed linear drift of spiral waves in a wide range of light intensities.

DOI: 10.1103/PhysRevE.106.024405

I. INTRODUCTION

Spiral waves occur in various excitable media in chemical, physical, and biological systems. They have been found in the cardiac tissue [1], during the aggregation of slime mold amoebae [2], in the Belousov-Zhabotinsky (BZ) reaction [3], and in the catalytic oxidation of CO on a Pt(110) surface [4].

Spiral waves organize spatial excitation patterns and their dynamics determine important processes in excitable media. For example, stationary rotating spiral waves in the heart are responsible for an arrhythmia called monomorphic tachycardia [5], while their breakup causes ventricular fibrillation [6,5], which is the main cause of sudden cardiac death [7]. A special type of dynamics is the drift of spiral waves. It was shown that the drift of spiral waves in the heart is responsible for a dangerous cardiac arrhythmia called polymorphic ventricular tachycardia [8]. Also, directed drift can be used to control the position of spiral waves in excitable media, for example, to bring them to the boundary and eliminate them. Therefore the methods to induce and control the drift of spiral waves are an important way to control their dynamics.

From theoretical studies, it is known that drift of stationary rotating spiral waves can occur as a result of spatial heterogeneity with respect to properties of nonlinear functions describing excitability [9,10], or due to heterogeneity in the spatial operator describing connections in excitable media. In the second case the drift often occurs as a result of additional gradient terms in the spatial operator [11–14]. These terms occur, for example, due to derivatives of the diffusion tensor if it changes in space, and they account for drift of spiral waves there [11]. Gradient terms occur in curvilinear coordinate systems linked to the filaments of three-dimensional (3D) spiral waves, and they account for curvature-dependent filament drift [12–14].

Such gradient terms also naturally occur in the case of some external actions on the excitable media. For example it was shown that a DC electric field in the BZ reaction causes spiral drift at a constant velocity proportional to the field magnitude at an angle with the field direction [15–17]. Mathematically the action of the electric field is described as additional gradient terms in the spatial operator [15].

Application of the electric field provides one of the most straightforward ways to induce the desired drift of spiral waves, as the direction and the amplitude of the electric field are easy to change and control. Unfortunately, such an approach is impossible to apply to cardiac tissue, as there the action of the external field to the heart does not result in the

*Corresponding author: Alexander.Panfilov@UGent.be
†Corresponding author: hongzhang@zju.edu.cn

gradient terms in the equations describing cardiac propagation, due to the difference in the excitability mechanism. In this paper, we perform *in silico* studies and propose a method that solves such a problem for cardiac tissue. In particular, we show that similar action can be realized using the modern experimental technique of cardiac optogenetics. We show that it is possible to set up a feedback procedure in which some properties of the excitation pattern are extracted and then used to modulate a light intensity applied to optogenetic cardiac tissue. As a result, we obtain the same type of linear drift as in the BZ reaction with an applied external electric field. We study this process in detail and show how it depends on the excitability of cardiac tissue and the type of optogenetic action. In addition, we show that this approach can also be realized by a light source composed of discrete light-emitting diode (LED) sources and study how the spatial resolution of the sources affects the drift dynamics. We also show that such drift can eliminate spiral waves by their collisions with a boundary or result in the annihilation of counter-rotating spiral waves. Overall we propose a type of feedback procedure that can induce the linear drift of spiral waves in cardiac tissue and thus can be used to control their dynamics.

II. MODEL

A. FitzHugh-Nagumo model

The equation used in our two-component (u and v) reaction diffusion system is the FitzHugh-Nagumo (FHN) model [18,19]:

$$\frac{\partial u}{\partial t} = D\nabla^2 u + f(u,v) + I_{\text{optp}}, \tag{1a}$$

$$\frac{\partial v}{\partial t} = g(u,v), \tag{1b}$$

where $f(u,v) = (u - u^3/3 - v)/\varepsilon$, $g(u,v) = \varepsilon(u + \beta - \gamma v)$. u and v are the fast and slow variables, respectively. In this paper, we choose $D = 1$, $\varepsilon = 0.22$, $\gamma = 0.8$. In highly excitable medium, $\beta = 0.58$; in weakly excitable medium, $\beta = 0.78$.

The light-induced current I_{optp} in cardiac tissue can be depolarizing or hyperpolarizing [20–23]. In Eq. (1) a depolarized state corresponds to $u = u_{\max}$, while a resting (hyperpolarized) state corresponds to $u = u_{\min} = u_{\text{rest}}$. $u_{\max}$ and $u_{\min}$ are the upper and lower roots of $f(u, v_{\text{rest}}) = 0$, where v_{rest} is the value of v in the resting state. Thus we use $u = u_{\max}$ and $u = u_{\min}$ as a Nernst potential for the depolarizing and the hyperpolarizing current correspondently. Also we assume that the conductance of the optogenetic channels is g, which depends on the local light intensity at given point x, y and time t, and that we can control the value of g locally by light. For simplicity, we call g light intensity. Thus we get the following representations:

$$I_{\text{optp}}(x,y,t) = \begin{cases} I_{\text{depolarizing}} = -g(x,y,t)[u(x,y,t) - u_{\max}] \\ \text{or} \\ I_{\text{hyperpolarizing}} = -g(x,y,t)[u(x,y,t) - u_{\min}]. \end{cases} \tag{2}$$

Note that the light intensity is always positive, so $g \geqslant 0$, and for $u_{\min} < u < u_{\max}$ the depolarizing and the hyperpolarizing currents in Eq. (2) are positive (inward) and negative (outward), respectively.

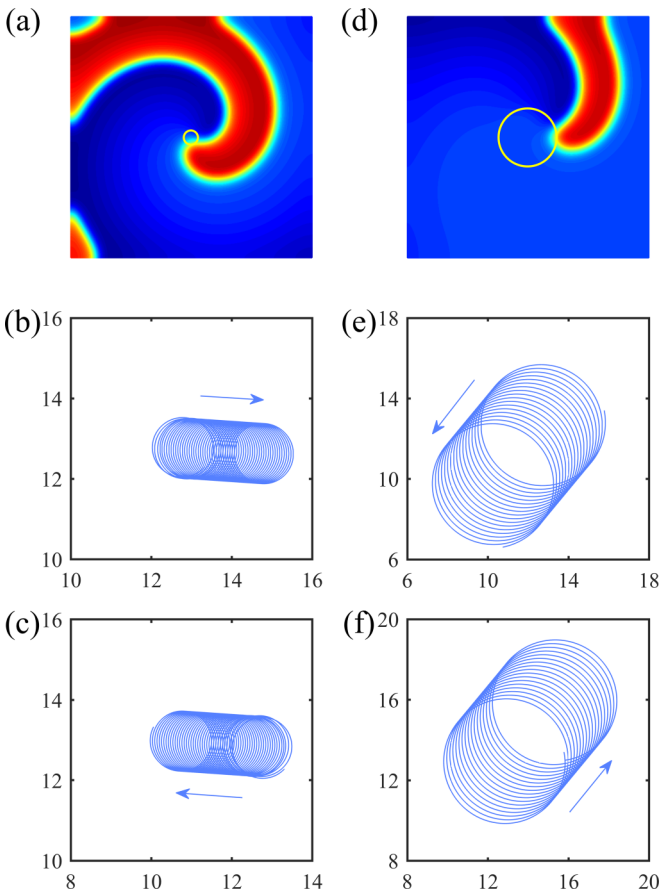

FIG. 1. Spiral waves dynamics under optical feedback. The shapes of spiral waves in highly (a) and weakly (d) excitable media without application of light. The wave in (a) or (d) rotates clockwise and the path of the spiral tip (yellow) is a circle, which is the core of the spiral wave. The color in (a), (d) shows the spatial distribution of the variable u with the red color corresponding to u_{excited} and the blue color corresponding to u_{rest}. Tip trajectories under the optical feedback given by Eq. (7) in highly (b) and weakly (e) excitable media. (c), (f) The same for the optical feedback given by Eq. (8). $g_o = 3.90625 \times 10^{-3}$, continuous light sources.

Simulations were performed in a medium of the size 25.6×25.6 in Figs. 1–7 for single rotating spiral waves and 51.2×51.2 in Figs. 8 and 9 for two counter-rotating spiral waves, corresponding to grids of 512×512 and 1024×1024, respectively, with the space step $\Delta x = \Delta y = 0.05$ and the time step $\Delta t = 0.0005$. All are in dimensionless space and time units.

B. Luo-Rudy model

We also implemented one of the most widely used realistic models for the membrane action potential, i.e., the Luo-Rudy model of mammalian ventricular cardiac tissue [24]:

$$\frac{\partial V}{\partial t} = -\frac{I_{\text{ion}} + I_{\text{optp}}}{C_m} + D\nabla^2 V, \tag{3a}$$

$$I_{\text{ion}} = I_{\text{Na}} + I_{\text{si}} + I_K + I_{K1} + I_{Kp} + I_b, \tag{3b}$$

where V is the transmembrane potential, $C_m = 1\,\mu\text{F/cm}^2$ is the membrane capacitance, and $D = 0.001\,\text{cm}^2/\text{ms}$ is the diffusion coefficient. I_{ion} contains six ionic currents: a fast sodium current I_{Na}; a slow inward current I_{si}; a time-dependent potassium current I_K; a time-independent potassium current I_{K1}; a plateau potassium current I_{Kp}; and a time-independent background current I_b. We considered a rigidly rotating spiral wave with the following parameter set: the maximum conductances of I_{Na}, I_{si}, I_K are $G_{\text{Na}} = 6\,\text{mS/cm}^2$, $G_{\text{si}} = 0.01\,\text{mS/cm}^2$, and $G_K = 0.423\,\text{mS/cm}^2$; the slow inactivation gate $j \equiv 1$. Simulations are performed in a medium of size $3 \times 3\,\text{cm}^2$ with the space step $\Delta x = \Delta y = 0.015\,\text{cm}$ and the time step $\Delta t = 0.005\,\text{ms}$. The spiral tip is defined by the intersection point of two $-35\,\text{mV}$ voltage contour lines with the time interval of 2 ms.

The optogenetic depolarizing current I_{optp} in Eq. 3(a) is described by a recent detailed four-state Markov light-sensitive Channelrhodospin-2 (ChR2) model [25,26] which is based on experimental measurements of this current [27]. This model is widely used in detailed studies on optogenetics in cardiology (see, e.g., Refs. [28–30]). The equation for the model is [27]

$$I_{\text{optp}} = g_{ChR2} G(V)(O_1 + \gamma O_2)(V - E_{ChR2}), \tag{4}$$

with

$$G(V) = \frac{10.6408\text{–}14.6408\exp(-V/42.7671)}{V},$$

$$\frac{dO_1}{dt} = -(G_{d1} + e_{12})O_1 + e_{21}O_2 + k_1 C_1,$$

$$\frac{dO_2}{dt} = e_{12}O_1 - (G_{d2} + e_{21})O_2 + k_2 C_2,$$

$$\frac{dC_1}{dt} = G_{d1}O_1 - k_1 C_1 + G_r C_2,$$

$$\frac{dC_2}{dt} = G_{d2}O_2 - (k_2 + G_r)C_2,$$

$$O_1 + O_2 + C_1 + C_2 = 1,$$

where $g_{ChR2} = 0.4\,\text{mS/cm}^2$ is the maximal conductance, $G(V)$ is the voltage-dependent rectification function, O_1, O_2, C_1, C_2 are the open and the closed state probabilities, $\gamma = 0.1$ is the conductance ratio of O_2/O_1, and $E_{ChR2} = 0\,\text{mV}$ is the reversal potential for ChR2. G_{d1}, G_{d2}, G_r, e_{12}, e_{21}, k_1, k_2 are kinetic parameters for the four-state Markov model:

$$G_{d1} = 0.075 + 0.043\tanh\left(-\frac{V+20}{20}\right),$$

$$G_{d2} = 0.05,$$

$$G_r = 4.34587 \times 10^{-5} \times \exp(-0.0211539274V),$$

$$e_{12} = 0.011 + 0.005\ln\left(1 + \frac{I_{\text{light}}}{0.024}\right),$$

$$e_{21} = 0.008 + 0.004\ln\left(1 + \frac{I_{\text{light}}}{0.024}\right),$$

$$k_1 = 0.8535 F p,$$

$$k_2 = 0.14 F p,$$

$$F = \frac{0.0006 I_{\text{light}}\lambda}{w_{\text{loss}}},$$

$$\frac{dp}{dt} = \frac{S_0 - p}{\tau_{ChR2}},$$

$$S_0 = 0.5\{1 + \tanh[120(100 I_{\text{light}} - 0.1)]\},$$

where I_{light} is the light intensity, $\lambda = 470\text{nm}$ is the wavelength of light, $w_{\text{loss}} = 0.77$ is the scaling factor for losses of photons, $\tau_{ChR2} = 1.3\,\text{ms}$ is the time constant of ChR2 activation, and F is the photon flux. p and S_0 are the state variables, denoting the time- and the light-dependent activation functions for ChR2, respectively.

III. RESULTS

A. Optical feedback system

To describe the effect of electric field on wave propagation in the BZ reaction, usually a term $-\vec{E}\cdot\nabla u$ is added to the equation for the diffusive species [15,31]. In the BZ reaction, spiral waves under a DC electric field ($\vec{E}$ is a constant) drift with a two-component velocity [15,16], one of which is parallel to the electric field and the other is perpendicular to it. The component perpendicular to the electric field changes its sign with the rotation direction of spiral waves.

To obtain a similar control effect in cardiac tissue we will use a special control scheme for light-induced current. For simplicity let us assume that $\vec{E}$ is directed parallel to the x axis. As the system has rotational symmetry, this is not a limitation. In this case, the DC electric field term in equations for chemical excitable media is $-E_x\partial u/\partial x$ and it has the following property: the sign of $-E_x\partial u/\partial x$ at each point in space is correlated with that of $\partial u/\partial x$. For example, if we apply an electric field along the positive x axis, i.e., $E_x > 0$, we have

$$\begin{aligned} -E_x\partial u/\partial x &\geqslant 0 \quad \text{if} \quad \partial u/\partial x \leqslant 0, \\ -E_x\partial u/\partial x &< 0 \quad \text{if} \quad \partial u/\partial x > 0. \end{aligned} \tag{5}$$

According to Eq. (2), we can reproduce the similar term in cardiac tissue equations for the FHN model if we consider a specific light-induced current in the following form:

$$I_{\text{optp}}(x, y, t) = \begin{cases} -g_o|\partial u/\partial x|(u - u_{\max}) \geqslant 0 & \text{if} \quad \partial u/\partial x \leqslant 0, \\ -g_o|\partial u/\partial x|(u - u_{\min}) < 0 & \text{if} \quad \partial u/\partial x > 0. \end{cases} \tag{6}$$

Here, we assume that the optical system produces a light that activates the optogenetic currents whose conductance is proportional to $|\partial u/\partial x|$ with a scaling factor g_o, and $u_{\min} < u < u_{\max}$. We use two types of light-induced current according to the sign of $\partial u/\partial x$. It means we apply the depolarizing current to the spiral pattern at points where the derivative $\partial u/\partial x$ is negative, and apply the hyperpolarizing current at sites where the derivative $\partial u/\partial x$ is positive.

Equation (6) constructs a feedback system that makes it possible for cardiac tissue under light to behave like chemical media under electric fields. Because a light feedback system

can have some operational time delay, we also consider a generalized term (7) in which the time delay τ is taken into account:

$$I_{\text{optp}}(x,y,t) = \begin{cases} -g_o|\partial u(t-\tau)/\partial x|(u(t)-u_{\max}) & \text{if } \partial u(t-\tau)/\partial x \leqslant 0, \\ -g_o|\partial u(t-\tau)/\partial x|(u(t)-u_{\min}) & \text{if } \partial u(t-\tau)/\partial x > 0. \end{cases} \tag{7}$$

For most of simulations we will use a small time delay $\tau = 0.01T$, where T is the spiral period.

If the electric field in chemical media is negative $E_x < 0$, we can adjust Eq. (7) by exchanging the polarizing currents:

$$I_{\text{optp}}(x,y,t) = \begin{cases} -g_o|\partial u(t-\tau)/\partial x|(u(t)-u_{\min}) & \text{if } \partial u(t-\tau)/\partial x \leqslant 0, \\ -g_o|\partial u(t-\tau)/\partial x|(u(t)-u_{\max}) & \text{if } \partial u(t-\tau)/\partial x > 0. \end{cases} \tag{8}$$

Equation (7) and (8) are schemes of the feedback control for the FHN model.

B. Optically induced drift of spiral waves

We study the tip trajectories of rigidly clockwise rotating spiral waves in the presence of the light-induced current in the form of Eq. (7). We considered cases of the highly and the weakly excitable media. This is because in Ref. [32] it is shown that spiral waves in highly and weakly excitable media drift in opposite directions in a DC electric field in chemical media.

Figures 1(a) and 1(d) show spiral waves and their cores, and Figs. 1(b) and 1(e) show the drift of spiral waves in the presence of the light-induced current in the form of Eq. (7). We see that the spiral waves undergo directional drift, and the drift has two direction components. One component is longitudinal directed along the direction of the "electric field" for highly excitable media or in the opposite direction for weakly excitable media. This is similar to the spiral wave drift induced by DC electric fields in a chemical medium (see Fig. 1 in [33]). There is also another transversal component, which depends on the rotation direction of the spiral wave. In Figs. 1(c) and 1(f), we perform similar simulations for the current given by Eq. (8) corresponding to the opposite direction of the electric fields in a chemical medium. We see that under an inverse "electric field" the spiral waves drift in the opposite direction [Figs. 1(c) and 1(f)].

Our optical feedback of Eqs. (7) and (8) uses both depolarizing and hyperpolarizing currents. It requires simultaneous expression in the cell of two different types of light-sensitive ion channels and the possibility to control them independently. This may be a challenging task. Thus, we also checked if our approach also works if only one type of ion channel is available. For that we propose two other possible realizations which rely only on the depolarizing or only on the hyperpolarizing current:

$$I_{\text{optp}}(x,y,t) = \begin{cases} -g_o|\partial u(t-\tau)/\partial x|(u(t)-u_{\max}) & \text{if } \partial u(t-\tau)/\partial x \leqslant 0, \\ 0 & \text{if } \partial u(t-\tau)/\partial x > 0, \end{cases} \tag{9}$$

where only the depolarizing current is used, or

$$I_{\text{optp}}(x,y,t) = \begin{cases} 0 & \text{if } \partial u(t-\tau)/\partial x \leqslant 0, \\ -g_o|\partial u(t-\tau)/\partial x|(u(t)-u_{\min}) & \text{if } \partial u(t-\tau)/\partial x > 0, \end{cases} \tag{10}$$

where only the hyperpolarizing current is used.

Figure 2 shows examples of the application of either the depolarizing current, Eq. (9), or the hyperpolarizing current, Eq. (10). We see that in both cases spiral wave drift is parallel to the "electric field" for highly excitable media and antiparallel to the "electric field" for weakly excitable media, which are the same as Figs. 1(b) and 1(e) where both currents are present. However, the drift in Fig. 2 occurs with slower speeds, and the ratio of the longitudinal to the transversal velocity components changes, which results in slightly different drift angles.

C. Discrete light sources

One of the possible practical realizations of the optical feedback system is a light source consisting of an array of computer-controlled LED sources. Such sources were developed for various applications in neuroscience (see, e.g., [34]) and cardiology [29,35,36], and many similar sources are currently under development. Light in such arrays is produced by individual LED sources, each of which is controlled separately by a computer and illuminates a small area.

We performed simulations that mimic the action of such light sources. We assume that each LED illuminates an area of 5×5 grid points and is controlled by our feedback given by Eq. (7), with the derivative $\partial u/\partial x$ measured at the center point. Figure 3 shows how the proposed optical feedback affects the tip trajectory for such discrete sources containing different numbers of LED sources (keep LEDs $\times\, g_o =$ constant). We see that the drift remains straight when the

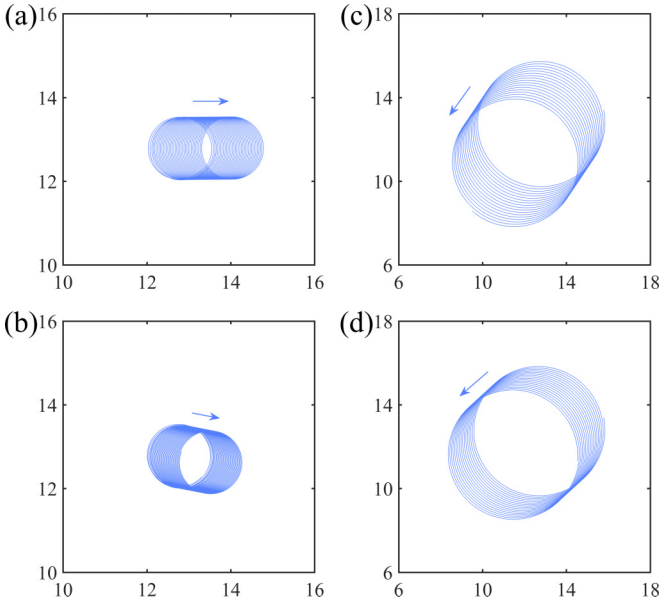

FIG. 2. The drift of spiral waves when the optical feedback uses only depolarizing or hyperpolarizing current. (a), (c) Application of the depolarizing current given by Eq. (9). (b), (d) Application of the hyperpolarizing current given by Eq. (10). $g_o = 3.90625 \times 10^{-3}$, continuous light sources. (a), (b) Highly excitable media. (c), (d) Weakly excitable media.

number of LED is 32×32 [Figs. 3(a) and 3(d)], slightly curves when the number is 16×16 [Figs. 3(b) and 3(e)], and becomes not straight and twists when the number turns to 8×8 [Figs. 3(c) and 3(f)].

Thus for all cases the proposed feedback produces the drift of spiral waves and its longitudinal component has the same direction as for the continuous source. However, LEDs $=$ 16×16 [Figs. 3(b) and 3(e)] in our simulation is the minimum number of sources when we observe linear drift. We will use this number in our subsequent simulations.

In Fig. 4, we show how the time delay affects the drift dynamics. We see that for delays of both $0.02T$ and $0.05T$ the tip trajectories are almost the same as that of the time delay $0.01T$. [Compare Figs. 4(a), and 4(c) and Figs. 3(b) and 3(e).]

Figures 5 and 6 show the effect of the light intensity on the directional drift. We changed the total light intensity in two different ways. In Fig. 5 we fixed g_o at 0.04 and increased the number of sources from 16×16 to 32×32. We see that in this case the total drift speed V ($V = \sqrt{V_x^2 + V_y^2}$) linearly increases with the number of LEDs [Figs. 5(a) and 5(c)], while the drift angle remains unchanged [Figs. 5(b) and 5(d)].

In Fig. 6 we gradually increase g_o from 0.04 to 0.18 while keeping the total LED numbers unchanged (LEDs $= 16 \times 16$). We see that the drift speeds also linearly increase over g_o ranging from 0.04 to 0.18 [Figs. 6(a) and 6(c)], while the drift angles still keep unchanged [Figs. 6(b) and 6(d)].

D. Other types of induced dynamics

The spiral waves under the optical feedback drift along straight lines until they approach the boundary. If this drift is strong enough, spiral waves can collide with the boundary and

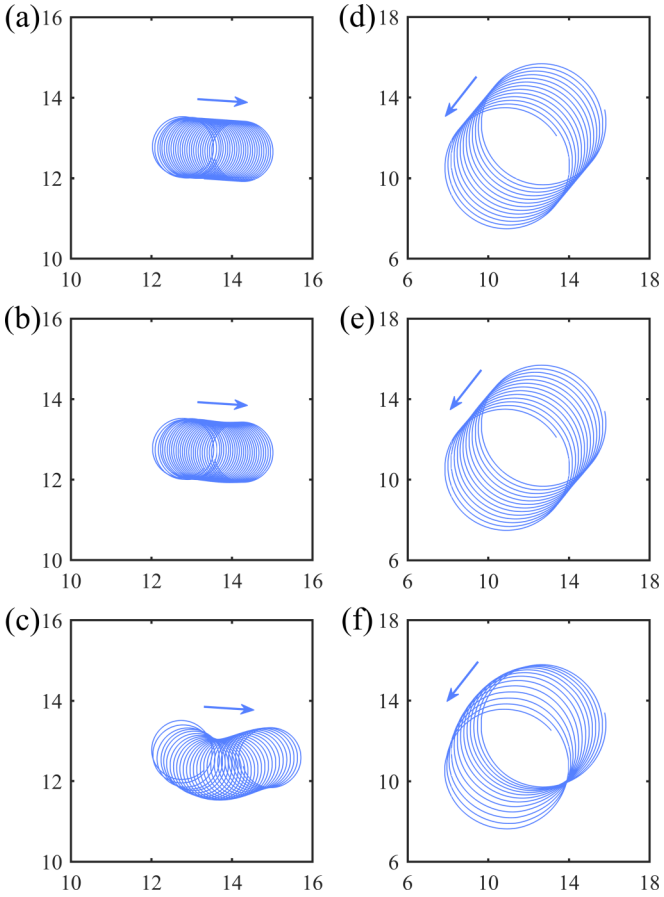

FIG. 3. Tip trajectories of spiral waves under discrete spot lights (LEDs). (a)–(c) Highly excitable media. (d)–(f) Weakly excitable media. (a), (d) LEDs $= 32 \times 32$, $g_o = 0.04$. (b), (e) LEDs $= 16 \times 16$, $g_o = 0.16$. (c), (f) LEDs $= 8 \times 8$, $g_o = 0.64$. The feedback is given by Eq. (7). Time delay $\tau = 0.01T$.

disappear. We illustrate this in Fig. 7 where we show that for both highly and weakly excitable media the optical feedback can remove spiral waves by their collisions with the boundary.

We also studied other wave sources. Figures 8 and 9 show the drift of two counter-rotating spiral waves which in cardiology are called figure-of-eight reentry. We consider highly excitable media in Fig. 8, weakly excitable media in Fig. 9, and two possible mutual orientations. We observe two types of dynamics. Under the light-induced current, the spiral waves either go apart [Figs. 8(a)–8(c) and 9(a)–9(c)], or move towards each other and annihilate [Figs. 8(d)–8(f) and 9(d)–9(f)]. These effects occur because the transversal component of the drift depends on the rotation direction of spiral waves, and for counter-rotating spiral waves it will have opposite directions. Thus this drift can either move spirals apart from each other as in Figs. 8(a)–8(c) and 9(a)–9(c) or bring them together as in Figs. 8(d)–8(f) and 9(d)–9(f).

E. Luo-Rudy model

The description for the optogenetic channelrhodopsin current used in the FHN model has substantial limitations. First, in the FHN model we assumed that the reversal potential of the depolarizing and the hyperpolarizing currents corresponds

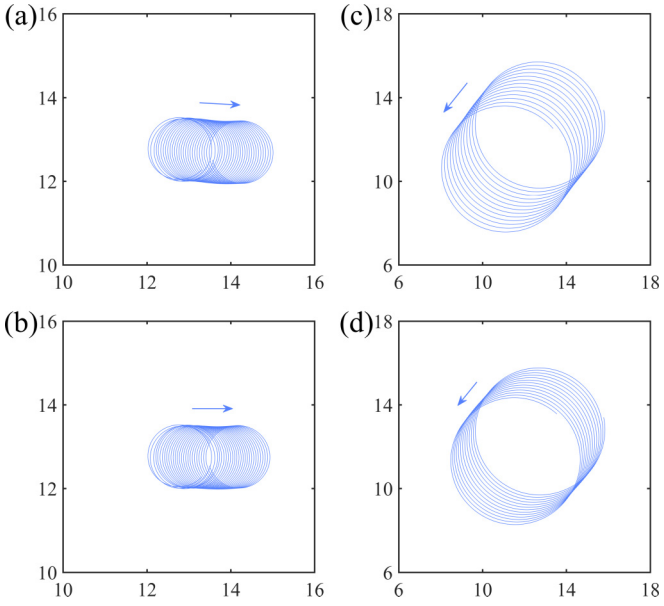

FIG. 4. Tip trajectories of spiral waves with longer time delay than that in Figs. 3(b) and 3(e): LEDs $= 16 \times 16$, $g_o = 0.16$. (a), (b) Highly excitable media. (c), (d) Weakly excitable media. (a), (c) Time delay $\tau = 0.02T$. (b), (d) Time delay $\tau = 0.05T$. The feedback is given by Eq. (7).

to the maximal and the minimal values for voltage. However, in reality they do not exactly coincide. Also we assumed instantaneous change in conductivity due to light; however, in reality the conductance change is a function of time. In order to check if our conclusions hold for biophysically motivated cardiac channelrhodopsin models, we performed additional studies in which we used the most accepted experimentally based model for the depolarizing channelrhodopsin current [36], which we included in the Luo-Rudy biophysical model for cardiac cells. Details on the implementation of the model are given in the model section.

In the Luo-Rudy model, our scheme of feedback light for ChR2 depolarizing current is

$$I_{\text{light}} = \begin{cases} I_o|\partial V(t-\tau)/\partial x| & \text{if } \partial V(t-\tau)/\partial x \leqslant 0, \\ 0 & \text{if } \partial V(t-\tau)/\partial x > 0, \end{cases} \tag{11}$$

where $\tau = 0.01T$, T is the spiral period in the Luo-Rudy model, and I_o is the scaling factor of light intensity. The feedback light I_{light} in Eq. (11) is a direct analogue of the feedback current of Eq. (9) in the FHN model.

We used parameters which produce a rigidly rotating spiral, which together with tip trajectories are shown in Fig. 10(a). Figures 10(b)–10(f) show examples of spiral drift in the Luo-Rudy model with a feedback control given by Eq. (11) for five values of $I_o = (3, 5, 10, 20, 80) \times 10^{-5}$. In all these cases, we eventually observed drift along a straight line; however, for the case of smaller light intensity it occurred after some transient time [Fig. 10(b)]. Figures 10(d)–10(f) also show that the spiral wave can annihilate at boundary if $I_o \geqslant 10 \times 10^{-5}$ (similar to Fig. 7 of the FHN model). We also expect the same annihilation of two counter-rotating spirals in the Luo-Rudy model, which was observed in the FHN model (Figs. 8 and 9).

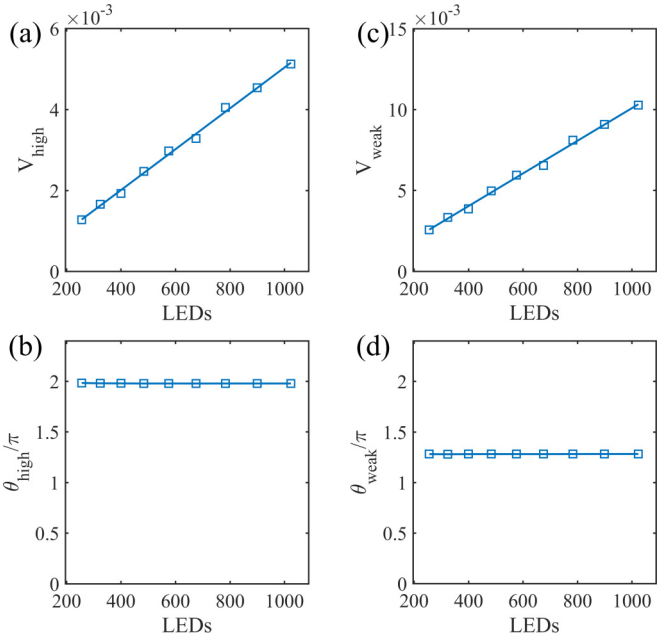

FIG. 5. The effect of the total light intensity on the drift speeds and directions. The light intensity was changed by increasing the number of LEDs. The feedback is given by Eq. (7). (a), (c) Relationships between the drift speeds and the LED numbers. (b), (d) Relationships between the drift angles and the LED numbers. (a), (b) Highly excitable media. (c), (d) Weakly excitable media. $g_o = 0.04$, LEDs : $16 \times 16, 18 \times 18, \ldots, 30 \times 30, 32 \times 32$.

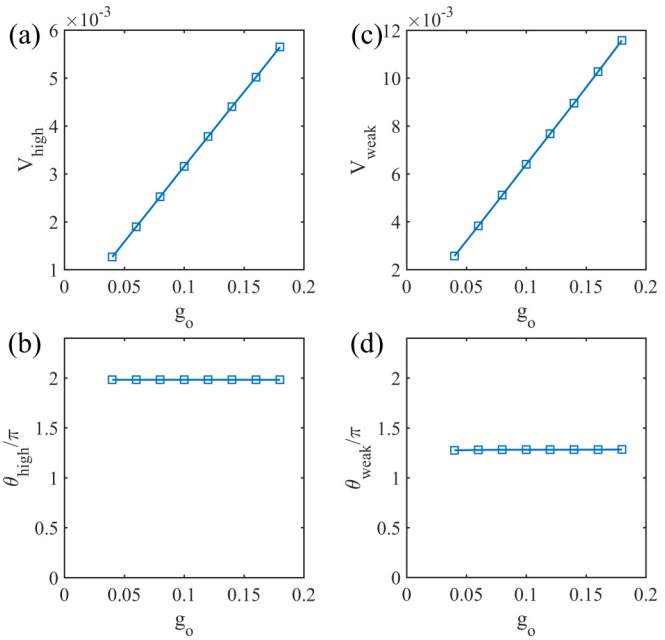

FIG. 6. The effect of the total light intensity on the drift speeds and directions in 16×16 LED arrays and the feedback is given by Eq. (7). The light intensity was changed by increasing g_o. (a), (c) Relationships between the drift speeds and g_o. (b), (d) Relationships between the drift angles and g_o. (a), (b) Highly excitable media. (c), (d) Weakly excitable media.

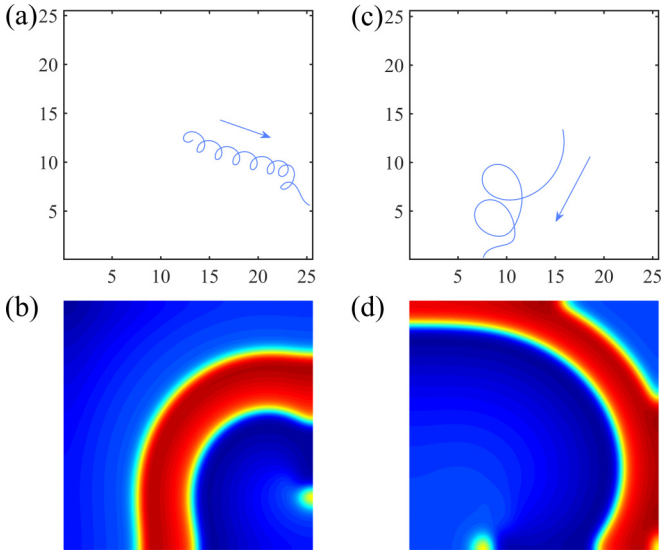

FIG. 7. Spiral waves drift and annihilate at the boundary under the optical feedback control Eq. (7) with $g_o = 0.12$, continuous light sources. (a), (b) Highly excitable media. (c), (d) Weakly excitable media. (a), (c) The initial patterns of the spirals are the same as in Figs.1(a) and 1(d).

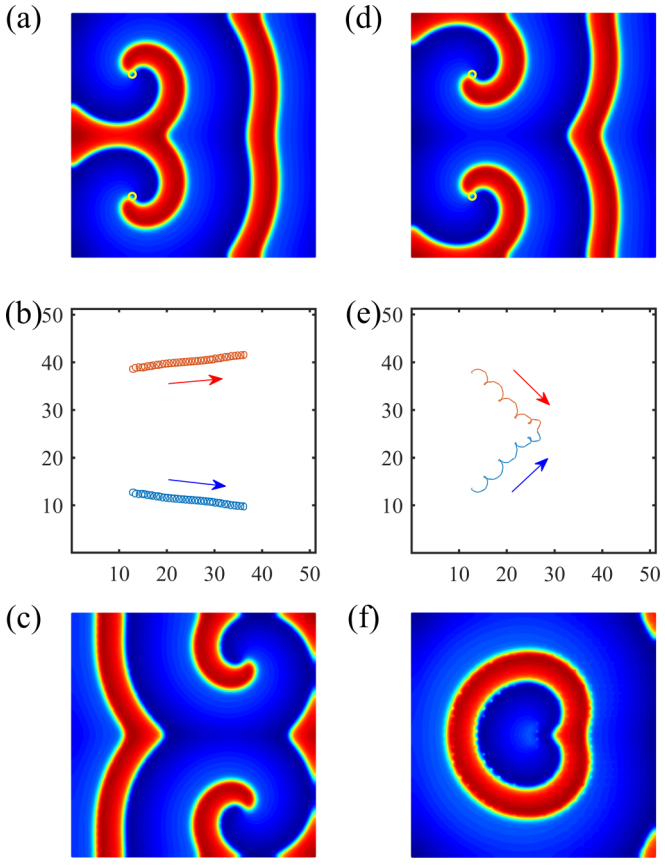

FIG. 8. Dynamics of two counter-rotating spiral waves under the optical feedback Eq. (7) in highly excitable media. (a)–(c) Two counter-rotating spiral waves move apart. $g_o = 2$, LEDs $= 32 \times 32$. (a) $t = 0$. (b) Tip trajectories. (c) $t = 400$. (d)–(f) Annihilation of spiral waves. $g_o = 18$, LEDs $= 32 \times 32$. (d) $t = 0$. (e) Tip trajectories. (f) Annihilation at $t = 57$.

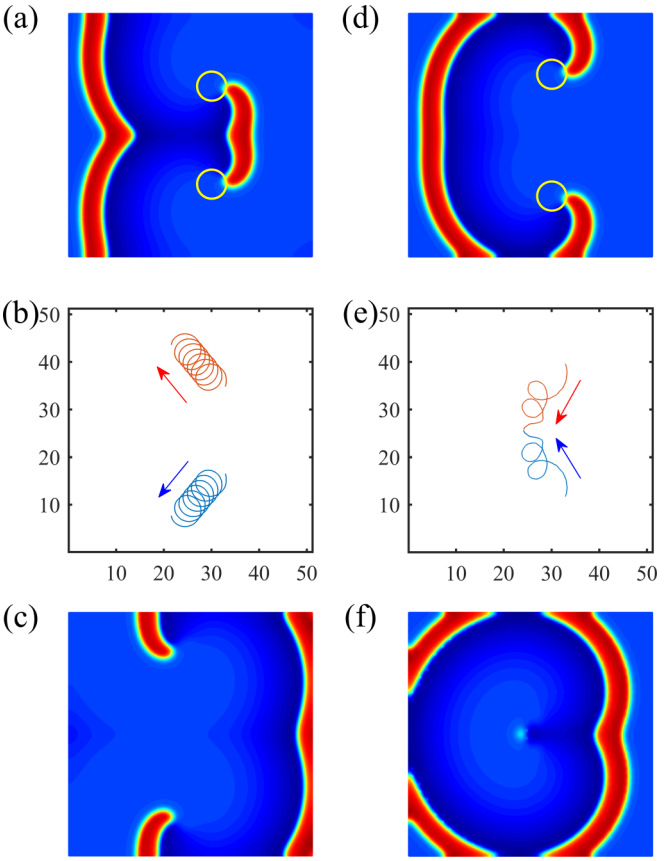

FIG. 9. Dynamics of two counter-rotating spiral waves under the optical feedback Eq. (7) in weakly excitable media. (a)–(c) Two counter-rotating spiral waves move apart. $g_o = 1$, LEDs $= 32 \times 32$. (a) $t = 0$. (b) Tip trajectories. (c) $t = 150$. (d)–(f) Annihilation of spiral waves. $g_o = 5$, LEDs $= 32 \times 32$. (d) $t = 0$. (e) Tip trajectories. (f) Annihilation at $t = 52$.

In our model the light intensity I_{light} is given by the product of I_o and $|\partial V/\partial x|$. Let us estimate the maximum light intensity which should be produced by our control system. From the relationship between I_o and I_{light} it follows that

$$(I_{\text{light}})_{\max} = I_o |\partial V/\partial x|_{\max}. \tag{12}$$

We record the maximum $|\partial V/\partial x|$ that occurred during simulations of Fig. 10, and obtain $|\partial V/\partial x| < 1.59 \times 10^3 < 1600\,(\text{mV/cm})$. Then, we use $|\partial V/\partial x|_{\max} = 1600\,(\text{mV/cm})$ and estimate the maximum light intensity in each simulation. The maximum light intensity I_{light} for different I_o is shown in the caption of Fig. 10.

From data shown in Fig. 10 we can conclude the following: our method works for all used intensities of the light. Also, all intensities are realistic: in Fig. 10, the maximum intensity $(I_{\text{light}})_{\max} = 1.28\,\text{mW/mm}^2$, which is more than four times lower than the maximum intensity $5.5\,\text{mW/mm}^2$ of experimental studies used to construct the ChR2 model [27].

IV. DISCUSSION

In this paper, we propose an algorithm for the feedback control of spiral waves in cardiac tissue. The proposed scheme uses optical feedback and can be applied to cardiac tissue in

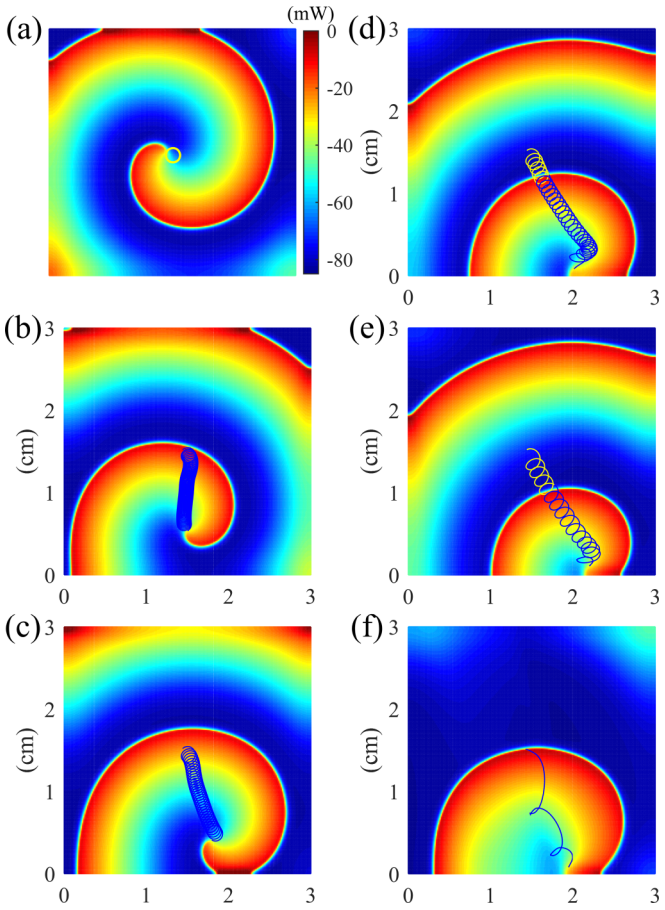

FIG. 10. Spiral wave dynamics in the Luo-Rudy model with continuous light sources. Color coding shows the potential V. (a) The shapes of rigidly rotating spiral wave and its core without application of light. (b)–(f) End time patterns and tip trajectories of spiral with different light intensity. (b) The spiral drift with long transient time when the light is small. $I_o = 3 \times 10^{-5}$, $(I_{\text{light}})_{\text{max}} = 0.048\,\text{mW/mm}^2$, $t = 2500\,\text{ms}$. (c) The spiral drift with $I_o = 5 \times 10^{-5}$, $(I_{\text{light}})_{\text{max}} = 0.08\,\text{mW/mm}^2$, $t = 1500\,\text{ms}$. (d) The spiral annihilates at the boundary when the drift becomes stronger. $I_o = 10 \times 10^{-5}$, $(I_{\text{light}})_{\text{max}} = 0.16\,\text{mW/mm}^2$, $t = 1242\,\text{ms}$. (e) The spiral drift faster with $I_o = 20 \times 10^{-5}$, $(I_{\text{light}})_{\text{max}} = 0.32\,\text{mW/mm}^2$, $t = 675\,\text{ms}$. (f) The drift with large light intensity. $I_o = 80 \times 10^{-5}$, $(I_{\text{light}})_{\text{max}} = 1.28\,\text{mW/mm}^2$, $t = 152\,\text{ms}$.

which photosensitive ion channels or pumps are introduced. We show that if we modify the conductance of ion channels based on the spatial derivatives of the transmembrane potential we can induce linear drift of spiral waves in cardiac tissue. Using the generic FHN model we show that the method works for the depolarizing optogenetic current, the hyperpolarizing current, and if both the depolarizing and the hyperpolarizing photosensitive currents are present. Note that although the effect is most pronounced when both the depolarizing and the hyperpolarizing photosensitive currents are present, experimentally it is very challenging to express in real cells for both currents and also to control them independently. Because most of the current experimental research was performed for a depolarizing photosensitive current [21] we extend our study and perform additional simulations using a biophysical model for cardiac cells in which we included the most accepted experimentally based model for the depolarizing photosensitive current. We show that in this case our method also induces stable linear drift of spiral waves for realistic intensities of the applied light.

In this paper we used a two-dimensional (2D) representation of cardiac tissue. Such a representation can properly reproduce processes which occur in cardiac cell cultures [21], or atria of the heart, which have thin walls. However, the ventricles of the heart have thick walls, and to study effects of our control procedure there one needs to perform simulations in 3D cardiac models, such as those in Refs. [37,20]. Note that in 3D many additional factors may affect our control procedures. First of all, the optogenetic signal influences only the surface of the heart. More specifically, for activation of optogenetic current the light needs to be delivered at a given location. Due to scattering, the light intensity reduces when light propagates inside cardiac tissue. In study [20] it was estimated that the optogentic effect can be observed only for a layer of thickness of about 1.5 mm. Also, the intensity of the light in that case will not be constant, but will reduce with the thickness by the exponential law [20]. Because the thickness of ventricles of the heart is between 6 and 12mm, the control signal will influence only 12–25% of the total thickness of the tissue. As a result, the control procedure will likely be able to affect only a part of the filament of a 3D spiral wave (scroll wave). It is also important to consider additional 3D effects of its own filament dynamics. The most important of those is filament tension [12,38,39]. It was shown that the filament of a 3D spiral wave tends either to decrease its length, which is called the positive filament tension [12,39], or increase its length, which is called the negative filament tension [38,39]. The type of the dynamics depends on the parameters of the equation, e.g., excitability of cardiac tissue [38]. Simulations in the Luo-Rudy model showed that for most of parameter values the filament tension in cardiac tissue is positive, and in a very low excitability case it can become negative as well [40].

Based on known properties of filaments, we can expect the following dynamics of 3D spiral wave if we apply our control procedure. Let us assume that we initially have a 3D spiral wave with the filament extended from the inner surface of the heart, the endocardium, to the outer surface of the heart, the epicardium, and the filament is orthogonal to the surfaces. Let us apply our optical control procedure and illuminate the outer surface of the heart, the epicardium. The control procedure should work normally for the part of 3D spiral wave located close to the epicardium and thus cause drift as it was in our 2D simulations. However, as light will not penetrate through all the thickness of the heart, the control procedure will not affect the other part of 3D spiral wave located close to the endocardium. As a result, such drift will try to elongate the filament. Now consider the case of positive filament tension. Because in the positive tension case the filament will try to decrease its length, the tension will try to keep the length of the filament minimal and thus keep the filament orthogonal to the surfaces of the heart. Consequently, if the control procedure will cause strong drift of one part of the filament at the epicardium, the filament tension will "pull" its another part,

and the whole filament should drift in a similar way as in 2D. In contrast, for the case of negative filament tension, the filament tends to increase its length and thus the drift of one part of the filament should not induce the drift of the filament as a whole. Thus we expect that our method will work only for the positive filament tension case. It would be interesting to perform simulations of these phenomena, find out if our assumptions are correct, and quantify them.

V. CONCLUSION

In conclusion, we propose a method of optical feedback which induces directed linear drift of spiral waves in cardiac tissue. The method works for continuous and discrete light sources and for depolarizing and hyperpolarizing photosensitive ion channels. Using this method it is possible to displace effectively spiral waves in cardiac tissue, or remove them by collisions with the boundary or with each other.

ACKNOWLEDGMENTS

We thank D. Pijnappels, Q. H. Li, and Y. J. He for helpful discussions. This work was supported by the National Natural Science Foundation of China under Grants No. 12075203 and No. 12005066, and research at Sechenov University was financed by the Ministry of Science and Higher Education of the Russian Federation within the framework of state support for the creation and development of World-Class Research Centers "Digital Biodesign and Personalized Healthcare" 075-15-2020-926.

[1] J. M. Davidenko, A. V. Pertsov, R. Salomonsz, W. Baxter, and J. Jalife, Nature (London) **355**, 349 (1992).
[2] K. J. Lee, E. C. Cox, and R. E. Goldstein, Phys. Rev. Lett. **76**, 1174 (1996).
[3] A. T. Winfree, Science **175**, 634 (1972).
[4] S. Jakubith, H. H. Rotermund, W. Engel, A. von Oertzen, and G. Ertl, Phys. Rev. Lett. **65**, 3013 (1990).
[5] S. V. Pandit and J. Jalife, Circ. Res. **112**, 849 (2013).
[6] A. V. Panfilov and A. V. Holden, Phys. Lett. A **151**, 23 (1990).
[7] R. J. Myerburg, K. M. Kessler, A. Interian, Jr., P. Fernandez, S. Kimura, P. L. Kozlovskis, T. Furukawa, A. L. Bassett, and A. Castellanos, in *Cardiac Electrophysiology, From Cell to Bedside*, edited by D. P. Zipes, and J. Jalife (W. B. Saunders, Philadelphia, 1990), p. 666.
[8] R. A. Gray, J. Jalife, A. V. Panfilov, W. T. Baxter, C. Cabo, J. M. Davidenko, and A. M. Pertsov, Circulation **91**, 2454 (1995).
[9] A. N. Rudenko and A. V. Panfilov, Stud. Biophys. **98**, 183 (1983).
[10] K. H. W. J. Ten Tusscher and A. V. Panfilov, Am. J. Physiol. **284**, H542 (2003).
[11] H. Dierckx, E. Brisard, H. Verschelde, and A. V. Panfilov, Phys. Rev. E **88**, 012908 (2013).
[12] A. V. Panfilov, A. N. Rudenko, and V. I. Krinsky, Biofizica **31**, 850 (1986).
[13] J. P. Keener, Physica D **31**, 269 (1988).
[14] H. Verschelde, H. Dierckx, and O. Bernus, Phys. Rev. Lett. **99**, 168104 (2007).
[15] O. Steinbock, J. Schütze, and S. C. Müller, Phys. Rev. Lett. **68**, 248 (1992).
[16] K. I. Agladze and P. De Kepper, J. Phys. Chem. **96**, 5239 (1992).
[17] A. Belmonte and J.-M. Flesselles, Europhys. Lett. **32**, 267 (1995).
[18] R. FitzHugh, Biophys. J. **1**, 445 (1961).
[19] J. Nagumo, S. Arimoto, and S. Yoshizawa, Proc. IRE **50**, 2061 (1962).
[20] P. M. Boyle, J. C. Williams, C. M. Ambrosi, E. Entcheva, and N. A. Trayanova, Nat. Commun. **4**, 2370 (2013).
[21] R. A. B. Burton, A. Klimas, C. M. Ambrosi, J. Tomek, A. Corbett, E. Entcheva, and G. Bub, Nat. Photon. **9**, 813 (2015).
[22] R. Majumder, I. Feola, A. S. Teplenin, A. A. F. de Vries, A. V. Panfilov, and D. A. Pijnappels, eLife **7**, e41076 (2018).
[23] M. Funken, D. Malan, P. Sasse, and T. Bruegmann, Front. Physiol. **10**, 498 (2019).
[24] C. H. Luo and Y. Rudy, Circ. Res. **68**, 1501 (1991).
[25] P. Hegemann, S. Ehlenbeck, and D. Gradmann, Biophys. J. **89**, 3911 (2005).
[26] K. Nikolic, N. Grossman, M. S. Grubb, J. Burrone, C. Toumazou, and P. Degenaar, Photochem. Photobiol. **85**, 400 (2009).
[27] J. C. Williams, J. Xu, Z. Lu, A. Klimas, X. Chen, C. M. Ambrosi, I. S. Cohen, and E. Entcheva, PLoS Comput. Biol. **9**, e1003220 (2013).
[28] D. DeWoskin, J. Myung, M. D. C. Belle, H. D. Piggins, T. Takumi, and D. B. Forge, Proc. Natl. Acad. Sci. USA **112**, E3911 (2015).
[29] A. Klimas, C. M. Ambrosi, J. Z. Yu, J. C. Williams, H. Bien, and E. Entcheva, Nat. Commun. **7**, 11542 (2016).
[30] S. Hussaini, V. Venkatesan, V. Biasci, J. M. R. Sepulveda, R. A. Q. Uribe, L. Sacconi, G. Bub, C. Richter, V. Krinski, U. Parlitz, R. Majumder, and S. Luther, eLife **10**, e59954 (2021).
[31] V. Hakim and A. Karma, Phys. Rev. E **60**, 5073 (1999).
[32] V. Krinsky, E. Hamm, and V. Voignier, Phys. Rev. Lett. **76**, 3854 (1996).
[33] T. C. Li, X. Gao, F. F. Zheng, D. B. Pan, B. Zheng, and H. Zhang, Sci. Rep. **7**, 8657 (2017).
[34] N. McAlinden, Y. Cheng, R. Scharf, E. Xie, E. Gu, C. F. Reiche, R. Sharma, P. Tathireddy, M. D. Dawson, L. Rieth, S. Blair, and K. Mathieson, Neurophotonics **6**, 035010 (2019).
[35] O. J. Abilez, in *35th Annual International Conference of the IEEE Engineering in Medicine and Biology Society (EMBC)*, 3–7 July 2013, Osaka (IEEE, Piscataway, NJ, 2013).
[36] P. M. Bolye, T. V. Karathanos, and N. A. Trayanova, JACC Clin. Electrophysiol **4**, 155 (2018).
[37] R. H. Keldermann, K. H. W. J. ten Tusscher, M. P. Nash, C. P. Bradley, R. Hren, P. Taggart, and A. V. Panfilov, Am. J. Physiol. **296**, H370 (2009).
[38] A. V. Panfilov and A. N. Rudenko, Physica D **28**, 215 (1987).
[39] V. N. Biktashev, A. V. Holden, and H. Zhang, Philos. Trans. R. Soc. London Ser. A **347**, 611 (1994).
[40] S. Alonso and A. V. Panfilov, Chaos **17**, 015102 (2007).